ELSEVIER

Polymer 42 (2001) 3581–3587

polymer

www.elsevier.nl/locate/polymer

TTT cure diagram for an epoxy system diglycidyl ether of bisphenol A/1,2 diamine cyclohexane/calcium carbonate filler

L. Núñez*, F. Fraga, A. Castro, M.R. Núñez, M. Villanueva

Research Group TERBIPROMAT, Departamento de Física Aplicada, Universidad de Santiago 15706 Santiago de Compostela, Spain

Received 4 June 2000; received in revised form 30 June 2000; accepted 26 September 2000

Abstract

Curing reactions of the epoxy system consisting of a diglycidyl ether of bisphenol A (BADGE $n = 0$); 1,2 diaminecyclohexane (DCH); and calcium carbonate filler were studied to calculate a time–temperature-transformation (TTT) isothermal cure diagram for this system. Gel times were measured as a function of temperature using two experimental methods: solubility test and dynamic mechanical analysis (DMA). The results obtained are in fair agreement with that obtained for the two component system BADGE $n = 0/1,2$ DCH. Vitrification times for the three component system was higher than those obtained for the system BADGE $n = 0/1,2$ DCH and the conversions achieved were very close to maximum values. The activation energy for the overall polymerization reaction was calculated from the gel times obtained using the two above mentioned methods: solubility test (57.12 kJ/mol) and DMA (54.12 kJ/mol). These values are of the same order than those obtained for the two component epoxy system. It was established that the addition of calcium carbonate filler avoids the appearance of physical aging, thus making easier both the determination of glass transition temperatures, and the calculation of the TTT diagram.

Keywords: Epoxy-amine-filler reactions; Time–temperature-transformation diagram; Diffusion

1. Introduction

Curing reactions of thermoset materials originate a three-dimensional network after the chemical reaction of the epoxy resin and the appropriate hardener. During the cure process of a thermoset, the glass transition temperature (T_g) of the material increases as a consequence of an increase in the crosslinking density, and the molecular weight [1]. Because of this, there is a decrease in the free volume of both the epoxy groups and primary amine which have not reacted, due to the fact that some chains become hindered in an infinite molecular weight network. The transformation from a viscous liquid to an elastic gel is sudden and irreversible and marks the first appearance of the infinite network; it is called the gel point. Gelation is characteristic of thermosets, and it occurs at a well-defined and calculable stage in the course of the reaction, that is at specific values of conversion and T_g. One other phenomenon that may occur at any stage during cure is vitrification. This transformation from a viscous liquid or elastic gel to a glass begins to occur as the glass transition temperature of the system becomes coincidental with the cure temperature. The vitrification point marks a change in the reaction mechanism passing from a chemically kinetically-controlled stage to become diffusion-controlled. Samples vitrified during an isothermal curing ($T_g > T_c$) show an endothermic physical aging peak in the vicinity of T_g [2].

In this article a time–temperature-transformation (TTT) diagram is calculated for the epoxy system diglycidyl ether of bisphenol A (BADGE $n = 0$), 1,2 diaminecyclohexane (1,2 DCH), calcium carbonate, epoxy resin, curing agent, and inert filler, respectively. This diagram is compared to that calculated for the binary system BADGE $n = 0/1,2$ DCH [3], to check the influence of the filler on the curing process.

This diagram is a useful tool for designing of epoxy resins curing cycles, because all the phenomenological changes such as vitrification and gelation, char and isoconversion contours, including the maximum conversion curve are recorded on it. In a previous article, [4] a kinetic study of this epoxy system was reported. In this paper, we have concluded that the overall kinetic curing order is three and that experimental data better fitting corresponds to Kamal model accounting for the diffusion [5].

* Corresponding author. Tel./fax: +34-981-524350.
E-mail address: falisar1@uscmail.usc.es (L. Núñez).

0032-3861/01/$ - see front matter
PII: S0032-3861(00)00712-6

Table 1
Times and conversions at gel point from the solubility test

	Without filler Ref. [9]		With filler	
T (°C)	t_{gel} (min)	α	t_{gel} (min)	α
100	4.96	0.64	3.74	0.47
90	8.46	0.63	5.47	0.48
80	13.06	0.65	9.39	0.46
70	21.63	0.59	15.64	0.45
60	40.13	0.58	34.81	0.46

2. Experimental

2.1. Materials

The epoxy resin was a commercial BADGE ($n = 0$) (Resin 332, Sigma Chemical Co., St Louis, USA) with an equivalent molecular weight of 173.6 g/eq, as determined by wet analysis [6,7]. The curing agent was DCH (Fluka, Switzerland) with an amine hydrogen weight of 28.5. The inert filler was calcium carbonate (Analema, Spain).

2.2. Sample preparation

Epoxy resin and curing agent were carefully and homogeneously mixed by stirring the mixture under same conditions, at stoichiometric ratio, before adding 20% of the inert filler. The size of particle was 300 mesh, and the viscosity of the samples was measured using a gel-timer. In the first stages, no increase in the viscosity was observed with dispersion of the particles. For this reason, it was not necessary to use a dispersant to avoid flocculation of BADGE ($n = 0$). The 20% is refered to the total weight. All the products were mixed under a nitrogen atmosphere.

2.3. Techniques

A differential scanning calorimeter (DSC7) and a dynamic mechanical analyzer (DMA7) were used to obtain all the experimental data reported in this work.

For the determination of glass transition temperatures, a DSC7 was used in both dynamic and isothermal modes. Because of the wide range of temperature (−30–250°C), the calorimeter was calibrated using two standards indium and bidistilled water obtained by the milipore method. The size of the samples was 4–7 mg. All the experiments were carried out under a nitrogen atmosphere inside a DSC dry box at about 5°C. They were sealed using a press in aluminum pans before introducing them into the calorimeter.

Dynamic mechanical properties were measured using DMA7 operated in the parallel plate measuring system. The DMA was calibrated following the procedure given in the Perkin–Elmer DMA-7 manual. The DMA was calibrated using indium as a standard. Samples were under a constant dynamic force of 60 mN. The DMA was used also to measure the gel-times.

3. Results and discussion

3.1. Gelation study

Gelation is a transition taking place in the course of the curing reaction and is dependent on the stoichiometry, reactivity, and functionality of the reactants. Prior to gelation, the sample is soluble in some appropiate organic solvents; but after gelation, the system exhibits a rubbery viscoelastic behavior and an insoluble fraction appears which increases to the detriment of the soluble fraction.

The gel time is the time at which gelation occurs. This time can be experimentally determined using different methods: solubility test, gel-timer, DMA, etc. In the first stage of the present study, two methods were used: solubility test and DMA.

3.1.1. Solubility test

In this method, the time to reach a fibriform structure in tetrahydrofurane (THF) is measured [8]. The experimental procedure is as follows. A stainless steel can containing the sample was introduced into a thermostatted bath filled with polyethylene glycol. The sample was continuously shaken; and at different times, a part of the same was taken out from the container and poured into a beaker containing THF trying to determine the time necessary for the sample to become insoluble at which a fibriform structure is visualized. There is a difficulty in the application of this method to the epoxy system studied because as the material dissolves, the THF solvent becomes whitish because of $CaCO_3$, thus hindering the visualization of the fibriform structure formation. Six experiments were performed at every isothermal temperature, and the results obtained agree within 5%. However, this test was not considered a conclusive one, and to check results, gel times were also measured using the DMA method. After determination of the gel times corresponding to each isothermal temperature, the enthalpy values corresponding to each of these times were determined from the isothermal curves recorded during the calorimetric experiments. Each enthalpy value divided by the enthalpy value obtained from dynamic experiments gives gel conversion at every isothermal curing temperature (for more detail, see for example, Refs. [3,4).

Table 1 shows gel times and conversions obtained using the solubility test corresponding to the different isothermal temperatures for the two [9] and three (this article) component systems.

3.1.2. Dynamic mechanical analysis

DMA was used to measure dynamic mechanical properties of the epoxy. The equipment was operated in the parallel plate measuring system. Gel time was assigned as that corresponding to the maximum value of tan δ,[10] where δ is the phase angle between the imaginary part and the real part of the complex viscosity. Samples (10–20 mg) were placed in aluminum pans and covered with an aluminum

Table 2
Times and conversions at gel point from DMA experiments

	Without filler Ref. [9]		With filler		Gel-timer	
T (°C)	t_{gel} (min)	α	t_{gel} (min)	α	t_{gel} (min)	α
100	4.96	0.64	4.76	0.60	5.02	0.61
90	7.8	0.63	8.94	0.62	9.01	0.62
80	12.32	0.64	16.00	0.58	16.54	0.58
70	18.30	0.58	25.15	0.56	26.42	0.57
60	38.70	0.58	39.39	0.57	40.15	0.58

disk, which was pressed by a parallel plates platform till the disk was totally submerged in the sample. This procedure assures a good contact between the platform and the sample, thus improving the correctness of measurements. A quasi-isothermal regime can be achieved by cooling the sample up to 5°C below the experimental chosen temperature at a constant cooling rate of 0.1°C/min. Once the sample is inside the DMA furnace, the parallel plates experiment was programmed by means of a rounded point probe. As the DMA method employed for detection of gel point is questioned by several investigators, the experimental results obtained by this method were corroborated using a gel timer. The times obtained using this last method agree with DMA measurements within a 5%. For this reason, it was considered that the colloidal particles were well stabilized in the samples.

Table 2 shows gel times and conversions obtained using both DMA and gel-timer methods corresponding to the different isothermal temperatures for the two and three component systems.

As it can be seen in Table 1, gel times obtained from the solubility test for the two and three component systems widely differ. This fact could be associated to the lack of confidence of this method as a measurement technique for epoxy systems containing $CaCO_3$ as a filler. On the other hand, Table 2 shows gel times and conversions for the two epoxy systems obtained through the DMA method and with the gel-timer. As it can be seen, gel times obtained by these two methods are very similar to those obtained for the system without filler thus indicating that the presence of the filler does not influence the gel times. For the two component system, that is for the non-filled system, critical gel conversions are fairly in agreement with values predicted by Flory (58%)[11]. For the three component (filled) system, gel conversions also agree with those predicted by Flory [11]. Table 2 also shows a slight decrease in conversion with a temperature decrease, originated by the loss of crosslink as at low temperatures molecular motion decrease.

Table 3
Values of activation energies from solubility test and DMA experiments

	Without filler Ref. [9]		With filler		
	Solubility test	DMA	Solubility test	DMA	Gel-timer
E_a(kJ/mol)	52.88	51.42	57.12	54.15	53.48

The overall activation energy for the cure reaction process, can be obtained from gel time data, assuming that all reactions taking place during the curing process can be described through differential equations containing one unique apparent activation energy, E_a, according to the following equation [12,13]:

$$\frac{d\alpha}{dt} = A\, e^{-\frac{E_a}{RT}} f(\alpha), \tag{1}$$

where A is a constant, E_a is the apparent activation energy for the overall curing reaction, T is the isothermal curing temperature, and $f(\alpha)$ is a temperature independent function of conversion.

Integration of Eq. (1) from $\alpha = 0$ to $\alpha = \alpha_g$, and taking natural logarithms, gives

$$\ln \int_0^{\alpha_g} \frac{d\alpha}{f(\alpha)} = \ln A + \ln t_g - \frac{E}{RT}. \tag{2}$$

The left-hand side of this equation is temperature independent, so:

$$\ln t_g = \text{const} + \frac{E}{RT}. \tag{3}$$

The activation energy can be calculated as the slope of a $\ln t_g$ versus $1/T$ plot. Table 3 shows cure reaction activation energies for the two component system [9], and for the three component system (this work) obtained using gel times calculated through solubility test and DMA and gel-timer methods.

In this table, a better agreement for activation energies of both systems, calculated through DMA can be seen. This fact could be associated to the difficulty of measuring gel times using the solubility test. From these results, it can be assumed that the energy necessary for the beginning of polymerization is not influenced by the presence of the filler.

3.2. Vitrification study

In a DSC dynamic experiment, plots of dH/dT as a function of T show an endothermic step change in heat capacity at the glass transition. Glass transition temperature, T_g, is taken as the midpoint of this transition [14]. For a thermoset material, the glass transition temperature increases from an initial value, T_{g0}, (glass transition temperature of the prepolymer, or glass transition temperature corresponding to a null crosslinking) to a maximum value, $T_{g\infty}$, which corresponds to the fully cured material. Table 4 shows T_{g0} and $T_{g\infty}$ values for the filled [5] and non-filled systems [9]. It can be seen that $T_{g\infty}$ decreases for the filled system probably due to the loss of crosslinking because of the filler. However,

Table 4
Values of glass transition temperatures

	Without filler Refs. [3,9]	With filler
$T_{g\infty}$	146.3	127.6
T_{g0}	−30.1	−20.0

T_{g0} becomes less negative which could be caused by the rearrangement of the structure groups owing to the presence of a new component (the filler).

Fig. 1 shows T_g values as a function of the cure time, t_c, for the different isothermal cure temperatures. It can be seen that T_g rapidly increases with curing up to vitrification time of the material, at which $T_g = T_c$ [15]; then the increase in T_g becomes slower owing to diffusion effects. However, vitrification effects on curing reaction can be observed for $|T_c - T_g| = 20$ or 30°C [16] and for $T_c < T_{g\infty}$. In this sense, t_v denotes the time at which incipient vitrification takes place. For $t > t_v$, two different effects are associated with the further increase of T_g: on the one hand, conversion continues to increase, although at a greatly diminished rate; on the other hand, physical aging of the sample in the glassy state can appear as a consequence of T_g increase. Vitrification times, t_v, are shown in Table 5 for the system with and without filler at the different isothermal cure temperatures. It can be seen in this table, that the filled system needs more time to achieve vitrification at which conversions are very close to maximum values. This fact allows the

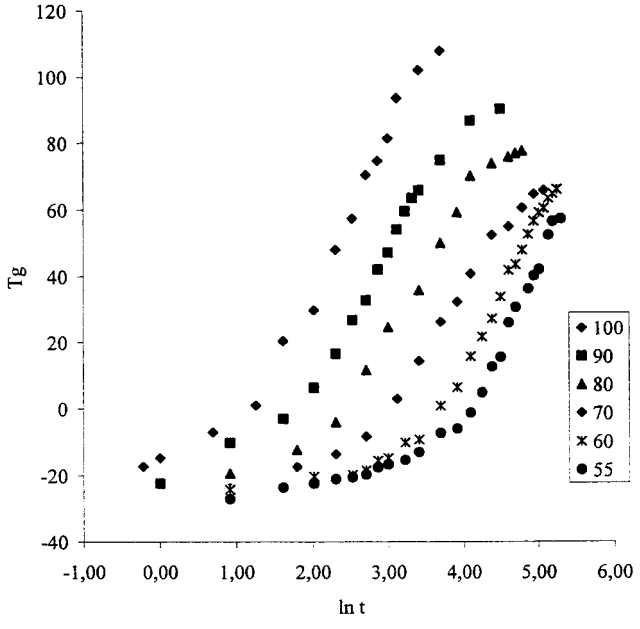

Fig. 1. T_g versus ln time for various cure temperatures from DSC isothermal cure experiments.

Table 5
Vitrification times at various isothermal cure temperatures

T	Without filler Ref. [3] t_v	With filler t_v
100	35.60	85.20
90	44.70	280.81
80	54.59	357.01
70	80.28	1282.43
60	186.00	2855.70
55	–	> 3000

performance of gradual and slower curing cycles, thus achieving high conversions before vitrification.

Fig. 2 shows a T_g versus α plot. In spite of the light dispersion of T_g data at high conversions, the existence of a relationship between T_g and conversion which is independent of the isothermal cure temperature can be confirmed. This relationship was also observed by some other authors [14,17]. In this way, T_g can be used as a reliable measure of conversion. This constitutes an important advance from the practical point of view since T_g can be measured more easily and with better accuracy than conversion, especially at high conversions at which T_g increases although the calorimeter does not show any change in the residual heat. Nielsen reported a modified form of the empirical DiBenedetto equation [15],

$$\frac{T_g - T_{g0}}{T_{g\infty} - T_{g0}} = \frac{\lambda\alpha}{1 - (1 - \lambda)\alpha}, \tag{4}$$

where T_{g0} is the T_g of the uncured monomer, $T_{g\infty}$ is the maximum glass transition temperature obtained experimentally for the fully cured material, and λ is taken as an adjustable structure-dependent parameter between 0 and 1. Fig. 3 shows a fit of T_g versus α using the DiBenedetto equation. In this equation λ is an adjustable parameter found to be $\lambda = 0.501$ [5]. Using the DiBenedetto equation and this calculated λ value, ${}_{gel}T_g$; that is the temperature at which gelation and vitrification occur simultaneously, was calculated to be ${}_{gel}T_g = 32.13$°C.

Values for λ and ${}_{gel}T_g$ calculated for the filled system widely differ from the values, $\lambda = 0.165$ and ${}_{gel}T_g = 7.2$°C, reported in a previous article [9] for the system without filler.

3.3. Time–temperature superposition of DSC data

A relationship between time and temperature can be established such that the behavior of the material for given time–temperature conditions is the same which could be achieved by different appropriate combinations of values of same variables. The theoretical basis for the superposition is the assumption that the polymerization is kinetically-controlled with a single apparent activation

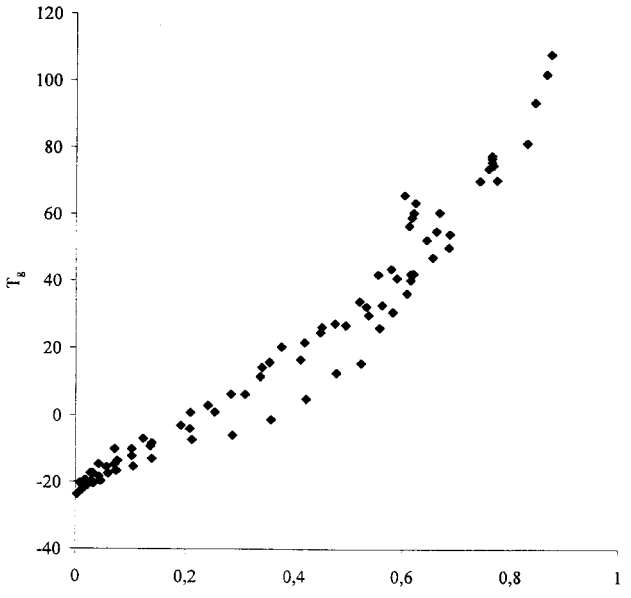

Fig. 2. One-to-one relationship between glass transition temperature (T_g) and conversion (α).

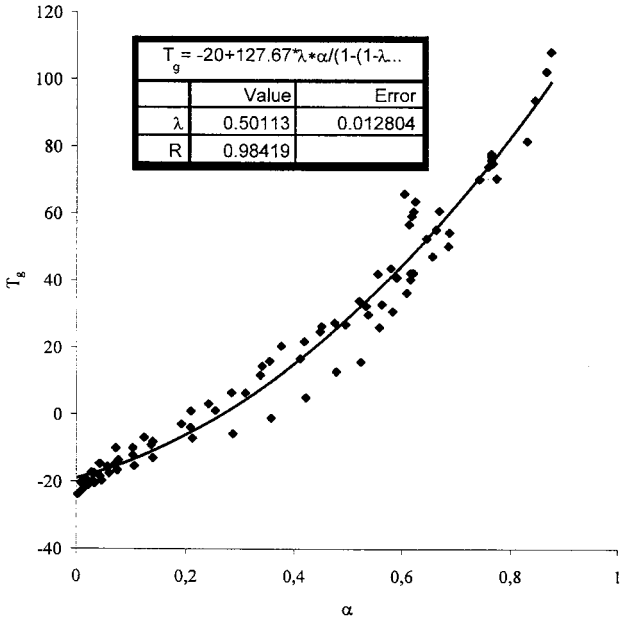

Fig. 3. One-to-one relationship between T_g and conversion using the DiBenedetto equation.

energy, and the existence of a one-to-one relationship between T_g and α [14,17]. This relationship allows the calculation of master curves at arbitrary reference temperatures. For this calculation, the knowledge of a relationship between reaction rate and conversion is necessary. Left-hand side in Eq. (2) only depends on conversion, and because there is a one-to-one relationship between T_g and conversion, some function of T_g, $F(T_g)$, can be substituted for the left-hand side of the equation, as follows:

$$F(T_g) = \ln A + \ln t_c - \frac{E}{RT_c}, \tag{5}$$

If T_c is substituted by any arbitrary reference temperature (T_r), gives:

$$F(T_g) = \ln A + \ln t_r - \frac{E}{RT_r}. \tag{6}$$

The shift factor, a_T, is the difference in ln time between two curves shifted at constant T_g (i.e. the same conversion):

$$a_T = \ln t_r - \ln t_c = \left(-\frac{E}{R}\right)\left(\frac{1}{T_c} - \frac{1}{T_r}\right). \tag{7}$$

Fig. 4 shows T_g versus ln t master curve at $T_r = 80$°C. From the master curve, values of T_g may be obtained at any T, providing the knowledge of T_g values corresponding to the cure reaction at a given reference temperature, T_r. In this plot, a deviation at high conversions can be observed. This deviation, usually caused by vitrification, which marks the onset of diffusion, was reported by some other investigators [14,16,18–20]. For this reason, the diagram cannot be extended into the diffusion-controlled regime since the master curve is only valid for kinetically-controlled regime.

Table 6 shows values of shift factor, a_T, at various isothermal temperatures for the system with and without filler for $T_r = 80$°C. This table shows no significant differences between a_T values for both systems. Because a_T depends Arrhenius-like on temperature, the activation energy for the polymerization reaction can be obtained as the slope of a a_T versus $1/T$ plot (Fig. 5). A value 54.4 kJ/mol for the activation energy was found to be in good agreement with the value obtained from gel time measurements.

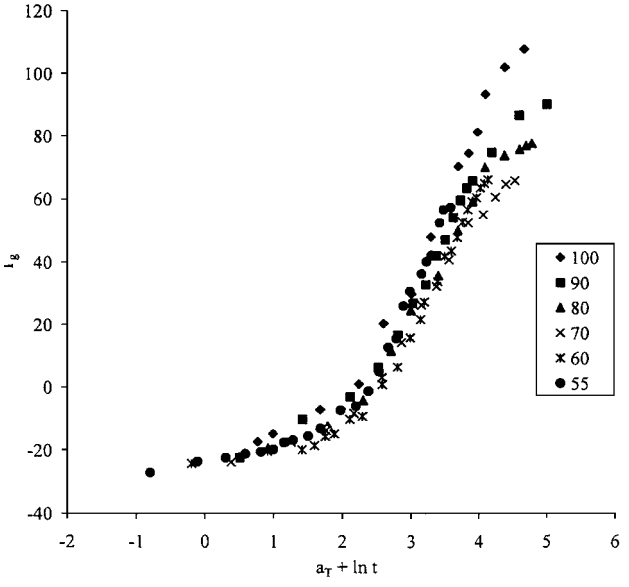

Fig. 4. T_g versus ln time for curve at a reference temperature $T_r = 80$°C.

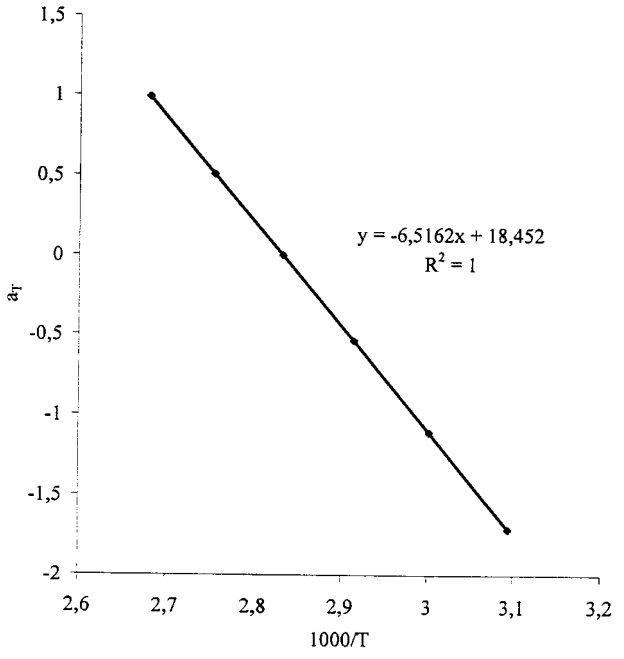

Fig. 5. Shift factor, a_T, versus 1000/T.

3.4. TTT diagram

The TTT isothermal cure diagram was calculated from the contours of the time to gel and to vitrify as a function of the reaction temperature (Fig. 6). Experimental data were fitted to curves, taking into account that the gelation and vitrification curves intersect at the curing time corresponding to ${}_{gel}T_g$. Isoconversion curves have been determined by numerical integration of the kinetic model accounting diffusion. Isoconversion curves corresponding to $\alpha = 0.30, 0.40,$

Table 6
Values of shift factor, a_T, at various isothermal cure temperatures

T	Without filler Ref. [3] a_T	With filler a_T
100	0.9	0.99
90	0.48	0.51
80	0.00	0.00
70	−0.51	−0.54
60	−1.05	−1.11
55	–	−1.71

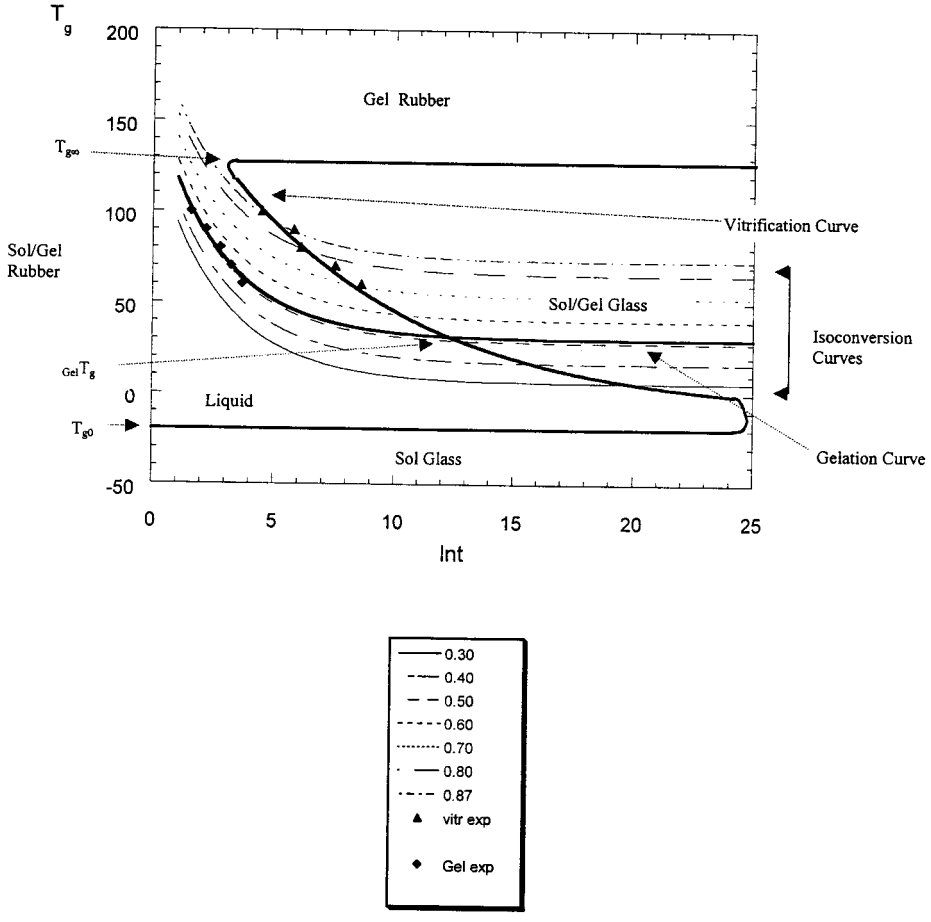

Fig. 6. Calculated TTT isothermal cure diagram for the system BADGE $n = 0/1,2$ DCH/$CaCO_3$.

0.50, 0.60, 0.70, 0.80, and 0.87 are plotted. The isoconversion curve 0.87 corresponds to the maximum achievable experimental extent of conversion.

An isothermal TTT diagram is characterized by three principal temperatures: T_{g0}, the initial T_g with null degree of conversion; ${}_{gel}T_g$ the temperature at which gelation and vitrification occur at the same time; and $T_{g\infty}$, the maximum glass transition temperature of the fully cured system. The values of the three characteristic temperatures were found to be −20, 32.13, and 127.6°C, respectively. This diagram shows the different stages experimented by a polymer material during the cure process. According to the TTT cure diagram, as a thermosetting material reacts, its glass transition temperature increases with the extent of conversion. When T_g reaches the value of the isothermal cure temperature, T_c, the material vitrifies. In the vicinity of vitrification the segmental mobility decreases, and the overall rate of reaction may become controlled by the limiting diffusion of reaction species [21]. The TTT diagram shown in Fig. 6 is similar to that reported by Chan et al.[21] for amine-rich systems. In this way, it can be considered that the behavior of a filled system is similar to that of an amine-rich epoxy system.

It was also observed during the TTT diagram calculation that the addition of the $CaCO_3$ filler hinders the appearance of physical aging.

4. Conclusions

A TTT diagram was calculated for the three component epoxy system BADGE ($n = 0$)/1, 2 DCH/$CaCO_3$ (filler) which shows some differences with the TTT diagram calculated for the non-filled system. Characteristic temperatures such as T_{g0}, ${}_{gel}T_g$, and $T_{g\infty}$ were determined. This TTT diagram is similar to others reported by some authors for amine-rich systems. The maximum achievable extent of reaction (0.87) is not very different from that corresponding to the non-filled system (0.96).

References

[1] Prime RB. In: Turi EA, editor. Thermal characterization of polymeric materials. San Diego: Academic Press, 1981.
[2] Wisanrakkit G, Gilllham JK. J Appl Polym Sci 1990;41:2885.
[3] Núñez L, Fraga F, Núñez MR, Villanueva M. J Appl Polym Sci 1998;70:1931.
[4] Núñez L, Fraga F, Castro A, Núñez MR, Villanueva M. J Appl Polym Sci 2000;75:291.
[5] Núñez L, Fraga F, Castro A, Núñez MR, Villanueva M. J Appl Polym Sci 2000;77:2285.
[6] Lee H, Neville K. Handbook of epoxy resin. NewYork: McGraw-Hill, 1967.
[7] May CA. Epoxy resins: chemistry and technology. New York: Marcel Dekker, 1988.
[8] Hagnaver GL. Chemorheology of thermosetting polymers. ACS Symposium Series, vol. 227. American Chemical Society, Washington DC, 1983.
[9] Núñez L, Taboada J, Fraga F, Núñez MR. J Appl Polym Sci 1997;66:1377.
[10] Gillham JK. Polym Engng Sci 1979;19:10.
[11] Flory PL. Principles of polymer chemistry. 15 ed. Ithaca, NY: Cornell University Press, 1992.
[12] Barton JM, Greenfield DCL, Hodd KA. Polymer 1992;33:1977.
[13] Oyanguren PA, Williams RJJ. J Appl Polym Sci 1993;47:1361.
[14] Simon SL, Gillham JK. J Appl Polym Sci 1992;46:1245.
[15] Pascault JP, Williams RJJ. J Polym Sci Polym Phys 1990;28:85.
[16] Dusek K. Advances in polymer science, vol. 78. Berlin: Springer, 1986.
[17] Simon SL, Gillham JK. J Appl Polym Sci 1993;47:461.
[18] Montserrat S. J Polym Sci Polym Phys 1994;32:509.
[19] Montserrat S. J Appl Polym Sci 1992;44:545.
[20] Montserrat S. J Therm Anal 1993;40:553.
[21] Chan LC, Nae HN, Gillham JK. J Appl Polym Sci 1984;29:3307.